Barrier and Mechanical Properties of Starch-Clay Nanocomposite Films

Xiaozhi Tang,[1] Sajid Alavi,[2,3] and Thomas J. Herald[1]

ABSTRACT

Cereal Chem. 85(3):433–439

The poor barrier and mechanical properties of biopolymer-based food packaging can potentially be enhanced by the use of layered silicates (nanoclay) to produce nanocomposites. In this study, starch-clay nanocomposites were synthesized by a melt extrusion method. Natural (MMT) and organically modified (I30E) montmorillonite clays were chosen for the nanocomposite preparation. The structures of the hybrids were characterized by X-ray diffraction (XRD) and transmission electron microscopy (TEM). Films were made through casting using granulate produced by a twin-screw extruder. Starch/MMT composite films showed higher tensile strength and better water vapor barrier properties than films from starch/I30E composites, as well as pristine starch, due to formation of intercalated nanostructure. To find the best combinations of raw materials, the effects of clay content (0–21 wt% MMT), starch sources (corn, wheat, and potato), and amylose content (≈0, 28, 55, 70, 100%) on barrier and mechanical properties of the nanocomposite films were investigated. With increase in clay content, significantly higher (15–92%) tensile strength (TS), and lower (22–67%) water vapor permeability (WVP) were obtained. The barrier and mechanical properties of nanocomposite films did not vary significantly with different starch sources. Nanocomposite films from regular corn starch had better barrier and mechanical properties than either high amylopectin or high-amylose-based nanocomposite films. WVP, TS, and elongation at break (%E) of the films did not change significantly as amylose content increased beyond 50%.

Plastics are widely used packaging materials for food and nonfood products due to desirable material properties and low cost. However, the merits of plastic packaging have been overshadowed by its nondegradable nature, thereby leading to waste disposal problems. The public is also gradually coming around to perceive plastic packaging as something that uses up valuable and scarce nonrenewable natural resources like petroleum. Moreover, the production of plastics is relatively energy intensive and it results in the release of large quantities of carbon dioxide as a by-product, which is often believed to cause, or at least contribute to, global warming. Some recent research findings have also linked plastic packaging to some forms of cancer (El Amin 2005; Kirsch 2005).

Packaging materials based on polymers that are derived from renewable sources may be a solution to the above problems. Such polymers include naturally existing proteins, cellulose, starches, and other polysaccharides, with or without modifications, and those synthesized chemically from naturally derived monomers such as lactic acid. These renewable polymers (or biopolymer) are not only important in the context of petroleum scarcity, but are also generally biodegradable under normal environmental conditions.

Interest and research activity in the area of biopolymer packaging films have been especially intensive over the past 10 years (Krochta and De Mulder-Johnston 1997; Tharanathan 2003). For food packaging, important characteristics include mechanical properties such as tensile strength and elongation at break (%E), and barrier properties such as moisture and oxygen permeabilities. To compete with synthetic plastics, biopolymer materials should have comparable mechanical or barrier properties. This is especially difficult with moisture barrier properties because of the hydrophilic nature of most biopolymers compared with hydrophobic synthetic polymers such as low-density polyethylene (LDPE). Moreover, mechanical and oxygen barrier properties of most biopolymer-based packaging materials are moderate to good at low relative humidity (rh), but deteriorate exponentially with increased rh (Krochta and De Mulder-Johnston 1997).

Among all biopolymers, starch is one of the leading candidates as it is abundant and cheap. The cost of the regular and specialty starches ($0.20–0.70/lb) compares well with that of synthetic polymers such as LDPE, polystyrene (PS), and polyethylene terephthalate (PET) ($0.50–0.75/lb) (Krochta and De Mulder-Johnston 1997). Moreover, starch is completely and quickly biodegradable and easy to process because of its thermoplastic nature (Doane 1994). Starch consists of two polysaccharides: linear amylose and highly branched amylopectin. The relative amounts of amylose and amylopectin depend on the plant source which affect the material properties and gelatinization behavior of the starch.

Many strategies have been developed to improve the barrier and mechanical properties of starch-based biodegradable packaging films. These include 1) addition of new plasticizers such as urea and formamide that aid in the thermoplastic process and also increase flexibility of the final product by forming hydrogen bonds with starch that replace the strong interactions between hydroxyl groups (Ma et al 2004); and 2) addition of synthetic biodegradable polymers like poly(vinyl alcohol) (PVOH) and polylactide (PLA) to produce materials with properties intermediate to the two components (Chen et al 1996; Ke and Sun 2000), resultant blends can be better processed by extrusion or film blowing and have mechanical and barrier properties superior to those of starch alone; and 3) addition of compatibilizers to lower the interfacial energy and increase miscibility of two incompatible phases, leading to a stable blend with improved characteristics (Mani et al 1998).

Recently, the application of polymer-layered silicate (PLS) nanocomposites has proven to be a promising option to improve barrier and mechanical properties (Sinha Ray and Okamoto 2003). Such PLS nanocomposites represent a new class of hybrid materials from inorganic silicate clays and organic polymer matrix. The clays used in PLS nanocomposites include montmorillonite (MMT), hectorite, saponite, and various modifications. These clays are environmentally friendly, naturally abundant, and economical. Like the better known minerals talc and mica, these layered silicates belong to the general family of 2:1 layered silicates (or phyllosilicates) (Giannelis 1996). Their crystal structure consists of layers made up of two silica tetrahedrals fused to an edge-shared octahedral sheet of either aluminum or magnesium hydroxide. Stacking of the layers leads to a regular van der Waals gap between the layers called the interlayer or gallery. In pristine layered silicates, the interlayer cations are usually hydrated Na^+ or K^+, showing hydrophilic surface properties.

For real nanocomposites, the clay layers must be uniformly dispersed in the polymer matrix (intercalated or exfoliated), as opposed to being aggregated as tactoids (Fig. 1).

[1] Food Science Institute, Kansas State University, Manhattan, KS 66506.
[2] Department of Grain Science & Industry, Kansas State University, Manhattan, KS 66506.
[3] Corresponding author. Phone: 1-785-532-2403. Fax: 1-785-532-4017. E-mail: salavi@ksu.edu

doi:10.1094/CCHEM-85-3-0433

The nanocomposites can be obtained by several methods including in situ polymerization, intercalation from solution, or melt intercalation (Sinha Ray and Okamoto 2003). Once clay intercalation or exfoliation has been achieved, improvement in properties can be manifested as an increase in tensile properties, as well as enhanced barrier properties, decreased solvent uptake, increased thermal stability, and flame retardance. A diverse array of polymers has been used in PLS nanocomposite formation, ranging from synthetic nondegradable polymers such as nylon (Kojima et al 1993a,b), polystyrene (Vaia et al 1995; Vaia and Giannelis 1997), and polypropylene (Kurokawa et al 1996; Usuki et al 1997) to biopolymers such as polylactide (Sinha Ray et al 2002a,b).

Several studies have been performed based on starch-clay nanocomposites. De Carvalho et al (2001) provided first insight to the preparation and characterization of thermoplasticized starch-kaolin composites by melt intercalation techniques. Park et al (2002 and 2003) reported an increase in %E and tensile strength by >20 and 25%, respectively, and a decrease in water vapor transmission rate by 35% for potato starch/MMT nanocomposites on addition of 5% clay. Wilhelm et al (2003) observed a 70% increase in tensile strength of Cará root starch/hectorite nanocomposite films at a 30% clay level. However, %E decreased by 50%. Very recently, Avella et al (2005) reported the preparation of potato starch/MMT nanocomposite films for food packaging applications. Results showed an increase in mechanical properties. Furthermore, the conformity of the resulting material samples with actual packaging regulations and European directives on biodegradable materials was verified by migration tests and by putting films into contact with vegetables and simulants. Pandey and Singh (2005) investigated different methods of preparing corn starch/MMT films and determined that the order of adding different components affected mechanical properties. Huang et al (2006) reported an increase in tensile strength and strain of corn starch/MMT nanocomposites by 450 and 20%, respectively, on addition of 5% clay. Chiou et al (2007) observed an improvement of thermal stability and water absorbance of wheat starch/MMT nanocomposites. Success of the studies above indicates that the clays show much promise in improving the barrier and mechanical properties of the starch-based packaging materials.

This study describes our attempts to fabricate starch-clay nanocomposites through melt-extrusion processing. We set out to investigate the influence of clay type (natural and organically modified clay), clay content, starch source, and amylose content on the formation of nanostructure and properties of the starch-clay composite films.

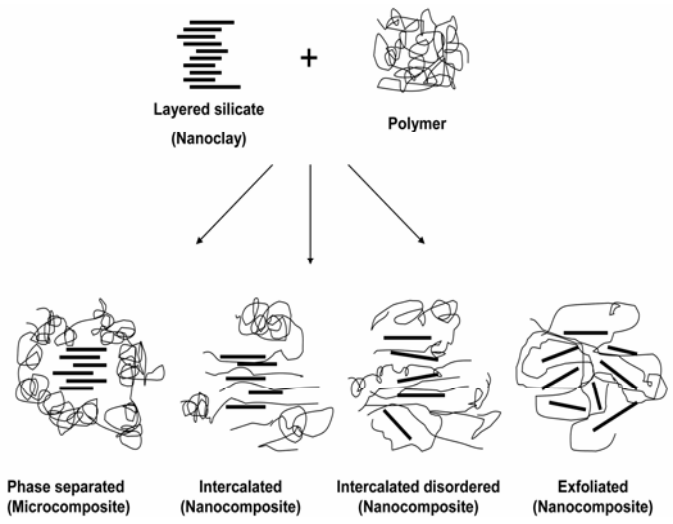

Fig. 1. Possible structures of nanocomposites.

MATERIALS AND METHODS

Materials

Two types of nanoclay were obtained from Nanocor (Arlington Heights, IL): natural montmorillonite (MMT) and onium ion modified MMT (Nanomer I30E). Regular corn starch, wheat starch, potato starch, and waxy corn starch were obtained from Cargill (Cedar Rapids, IA). High-amylose corn starches Hylon V (≈55% amylose), Hylon VII (≈70% amylose), and 100% amylose were obtained from National Starch (Bridgewater, NJ). Glycerol (Sigma, St. Louis, MO) was used as a plasticizer for all studies.

Starch-Nanoclay Composites

A laboratory-scale twin-screw extruder (Micro-18, American Leistritz, Somerville, NJ) with a six-head configuration and a screw diameter of 18 mm and L/D ratio of 30:1 was used for the preparation of starch-nanoclay composites. The screw configuration and barrel temperature profile (85-90-95-100-110-120°C) are shown in Fig. 2. Dry starch, glycerol (15 wt%), clay (0–21 wt%) and water (19 wt%) mixtures were extruded at a screw speed of 200 rpm. The extrudates were ground using a Wiley mill (model 4, Thomas-Wiley, Philadelphia, PA) and an Ultra mill (Kitchen Resource, North Salt City, UT) for further use.

X-ray diffraction (XRD) studies of the samples were conducted using a Bruker D8 Advance X-ray diffractometer (40kV, 40mA) (Karlsruhe, Germany). Samples were scanned at diffraction angle 2θ = 1–10° at a step of 0.01° and a scan speed of 4 sec/step. Transmission electron microscopy (TEM) studies were performed using a Philips CM100 electron microscope (Mahwah, NJ) operating at 100kV.

Films were made from ground extrudates by casting. Powders (4%) were dispersed in water and then heated to 95°C and maintained at that temperature for 10 min with regular stirring. Subsequently, the suspension was cooled to 65°C and poured onto petri dishes to make the films. The suspension in petri dishes was dried at 23°C and 50% rh for 24 hr, after which the films were peeled off for further testing.

Water vapor permeability (WVP) was determined gravimetrically according to the standard method E96-00 (ASTM 2000). The films were fixed on top of test cells containing a desiccant (silica gel). Test cells then were placed in a relative humidity chamber with controlled temperature and relative humidity (25°C and 75% rh). After steady-state conditions were reached, the weight of test cells was measured every 12 hr over three days. The water vapor transmission rate (WVTR) was determined as

$$\mathrm{WVTR} = \frac{\left(\frac{G}{t}\right)}{A}\ \mathrm{g/hr \times m^2} \quad (1)$$

where G = weight change (g), t = time (hr) and A = test area (m^2)

WVP was then calculated as

$$\mathrm{WVP} = \frac{\mathrm{WVTR} \times d}{\Delta p}\ \mathrm{g \times mm/kPa \times hr \times m^2} \quad (2)$$

where d = film thickness (mm) and Δp = partial pressure difference across the films (kPa).

Tensile properties of the films were measured using a texture analyzer (TA-XT2, Stable Micro Systems, UK) based on standard method ASTM D882-02 (ASTM 2002). Films were cut into strips 1.5 cm wide and 8 cm long and conditioned at 23°C and 50% rh for three days before testing.

Experimental Design and Statistical Analysis

WVP tests were replicated three times, while tensile tests were replicated five times. All the data were analyzed using scientific graphing and statistical analysis software (OriginLab, Northampton, MA). Statistical significance of differences was calculated using the Bonferroni LSD multiple-comparison method at $P < 0.05$.

RESULTS AND DISCUSSION

Structure of Starch-Nanoclay Composites

The XRD studies provided information on the intercalation and exfoliation processes and the short-range order of the molecular constituents in clay-polymer composites. It is generally thought that during the intercalation process, the polymer enters the clay galleries and forces apart the platelets, thus increasing the gallery spacing (*d*-spacing) (McGlashan and Halley 2003). According to Bragg's law, this would cause a shift of the diffraction peak toward a lower angle. As more polymers enter the gallery, the platelets become disordered and some platelets are even pushed apart from the stacks of clay particles (partial exfoliated). This will cause XRD peaks with a wider distribution or even further shift to the left side. TEM images provide further evidence for the occurrence of intercalation and exfoliation processes. TEM allows a qualitative understanding of the internal structure, spatial distribution, and dispersion of nanoparticles within the polymer matrix through direct visualization.

Figures 3 and 4 show the XRD patterns of composites with different nanoclay type and content. It should be noted that Lin (counts) refers to intensity of diffracted X-rays. It is clear that the dispersion states of nanoclays in the starch matrix depended on the type of clay used. The natural MMT exhibited a single peak at $2\theta = 7.21°$, whereas the starch/MMT hybrids showed prominent peaks at $2\theta = 4.98°$ (Fig. 3). Also, the starch blank (Fig. 3) exhibited a featureless curve in the range of 1–10° due to the amorphous character of gelatinized starch. The appearance of the new peak at 4.98° (*d*-spacing = 1.77 nm) with the disappearance of the original nanoclay peak at $2\theta = 7.21°$ (*d*-spacing = 1.23 nm) and increase of *d*-spacing indicated the formation of nanocomposite structure with intercalation of starch in the gallery of the silicate layers of MMT. The organically modified nanoclay I30E alone exhibited an intensive peak in the range of $2\theta = 3.93–4.16°$ (*d*-spacing ≈ 2.23 nm) (Fig. 4), whereas starch-I30E hybrids showed weak peaks just under the original peak of the I30E. This implied that little or no intercalation/exfoliation was achieved in the starch matrix.

The above results clearly showed that compatibility and optimum interactions between starch matrix, organic modifiers (if any), and the silicate layer surface were crucial to the formation of intercalated or exfoliated starch-layered silicate nanocomposites. Nanomer I30E is an onium ion surface modified montmorillonite mineral. Compared with natural MMT, I30E is more surface hydrophobic and therefore is not very miscible in the hydrophilic starch matrix. On the other hand, in natural MMT, due to the strong interactions between small amounts of polar hydroxyl groups of starch and glycerol and the silicate layers of the nanoclay (inorganic MMT Na^+), the starch chains and glycerol molecules can intercalate into the interlayers of the nanoclay.

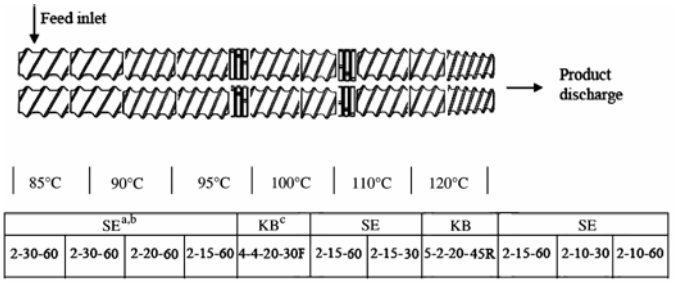

Fig. 2. Screw configuration and temperature profile for laboratory-scale extruder. Superscripts a) SE screw elements: number of flights – pitch (mm) – element length (mm) (2-30-60); b) all screws are forward and intermeshing; c) KB kneading block: number of disks – disk length (mm) – total block length (mm) – staggering angle of disks (F) or reverse (R) (4-4-20-45 F).

TEM micrographs of typical starch-MMT and starch-I30E composites are presented in Fig. 5. TEM results corresponded well with XRD patterns. Starch-MMT composites exhibited a multilayered nanostructure (Fig. 5A), whereas starch-I30E composites showed almost no intercalated morphology but instead had particle agglomerates or tactoids (dark spots in Fig. 5B).

Figure 6 shows the effects of clay content (<21 wt% MMT) on the structure of the nanocomposites. The only change was the intensity of peak, which increased with higher clay content. There was no shift in any of the peaks with varying clay contents, indicating that the clay content did not have any significant effect on the occurrence of intercalation or exfoliation. Figures 7 and 8 show the XRD patterns of 6 wt% MMT-based nanocomposites made from different starches. The data indicated that whatever the starch source (corn, wheat, or potato) or amylose content (≈0, 28, 55, 70, and 100%), complete disruption of the original nanolayer spacing of MMT was achieved, accompanied by starch-MMT intercalation at a higher *d*-spacing. Starch source or type did not have any effect on *d*-spacing of the nanocomposites. Although the MMT level was constant (6%) for all nanocomposites, interestingly, the intensity of the XRD peaks appeared to increase with amylose content with a maximum at 70% amylose. This may suggest the occurrence of partial exfoliation of clay platelets with the

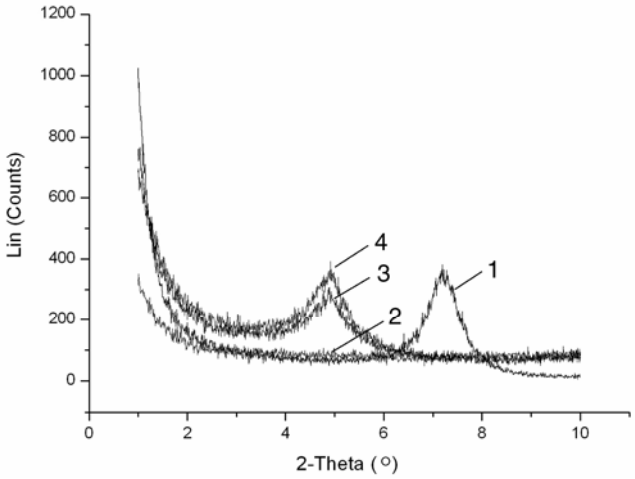

Fig. 3. XRD patterns of (1) natural montmorillonite (MMT), (2) corn starch blank (0% MMT), and (3 and 4) corn starch/nanoclay hybrids with 3 and 6% MMT, respectively.

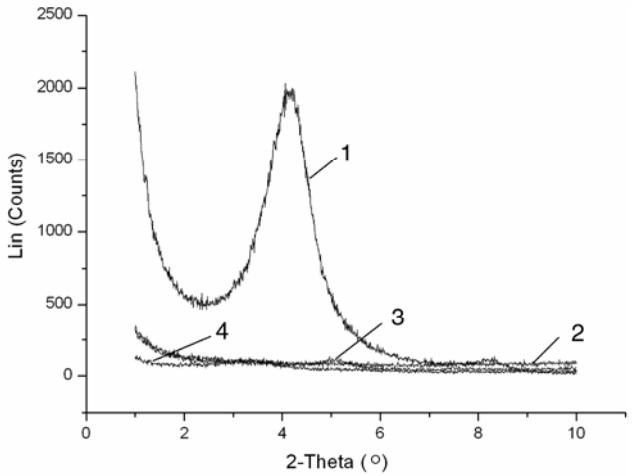

Fig. 4. XRD patterns of (1) original nanomer I30E, (2) corn starch blank (0% I30E), and (3 and 4) corn starch/nanoclay hybrids with 3 and 6% I30E, respectively.

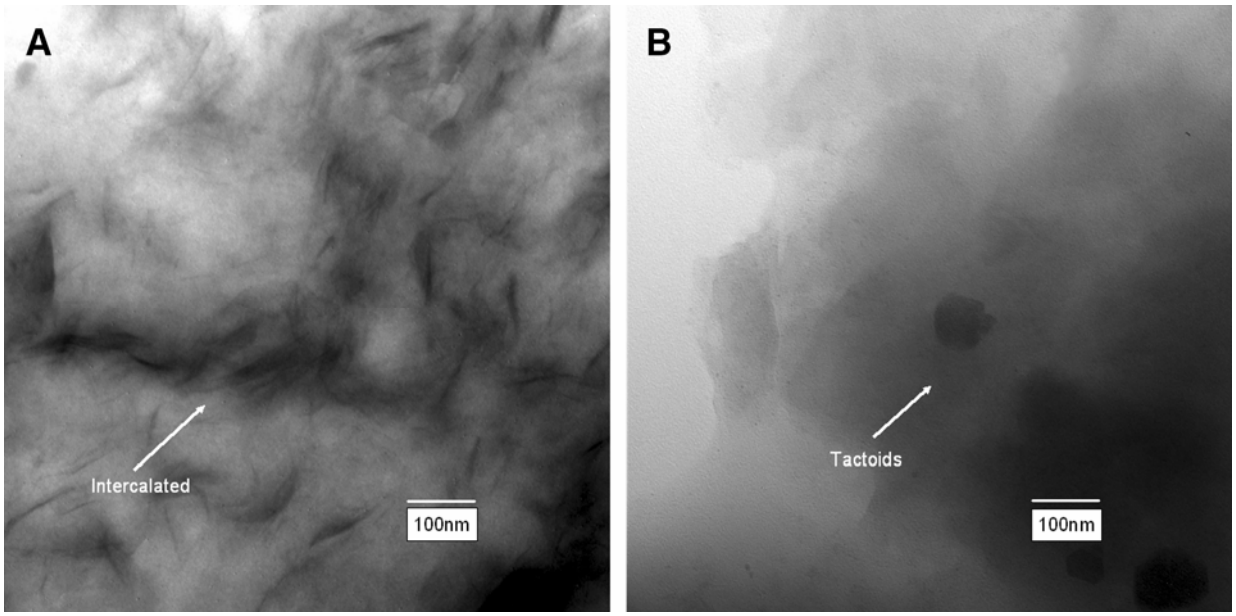

Fig. 5. TEM of (**A**) starch-6% MMT and (**B**) starch-6% I30E composites.

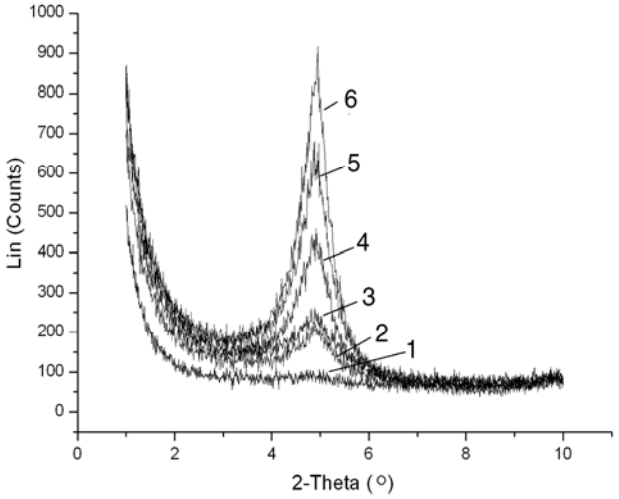

Fig. 6. XRD patterns of (1) wheat starch blank (0% MMT), and (2, 3, 4, 5, and 6) wheat starch-clay nanocomposites with 3, 6, 9, 15, and 21% MMT, respectively.

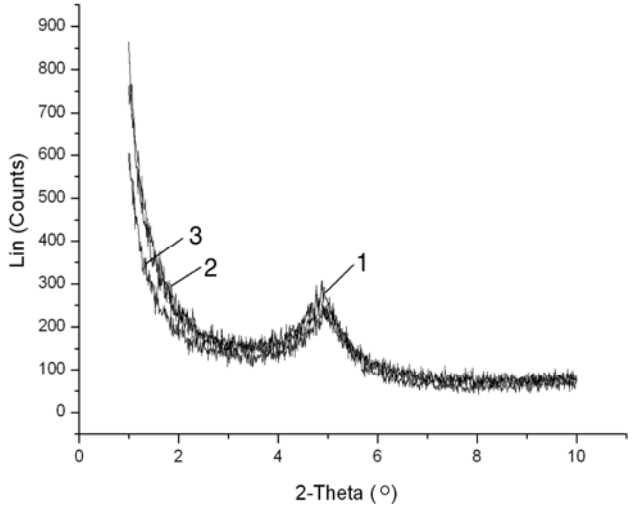

Fig. 7. XRD patterns of 6% MMT nanocomposites with (1) corn, (2) wheat, and (3) potato starches.

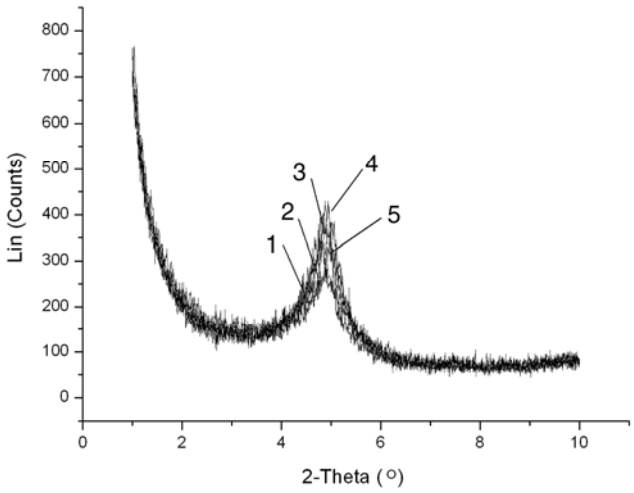

Fig. 8. XRD patterns of 6% MMT nanocomposites with (1) waxy corn starch, (2) regular corn starch, (3) Hylon V, (4) Hylon VII, and (5) 100% amylose.

penetration of starch biopolymers into the silicate layers leading to their dispersal. It was hypothesized that as amylose content increased to >50%, the degree of exfoliation decreased with more of the starch-MMT nanocomposite present in the intercalated state, leading to greater intensity of XRD peaks.

Water Vapor Permeability (WVP)

Tables I and II and Figs. 9 and 10 show the moisture barrier properties of the starch-nanoclay composite films. Water vapor permeability (WVP) of the films was examined at a difference of 0–75% rh across the films. Table I shows the effects of clay type on WVP of corn starch-based composite films. At the same clay level, WVP of the starch-MMT composite films was significantly lower than that of films made from starch-I30E composites. Second, there was no significant difference in WVP when the I30E content increased 0–9%, while WVP decreased significantly with the addition of 3–9% MMT. It was obvious that the addition of I30E did improve the barrier properties of the films, which indicated that improvement in film properties depended on the occurrence of intercalation or exfoliation (formation of nanocomposites).

TABLE I
Effects of Clay Type on WVP of Corn Starch-Based Films[a]

	WVP (g × mm/kPa × hr × m^2)	
Clay Content	**Starch-MMT**	**Starch-I30E**
0% clay	1.61 ± 0.08a	1.61 ± 0.08ae
3% clay	1.42 ± 0.04b	1.63 ± 0.12e
6% clay	1.06 ± 0.09c	1.58 ± 0.08e
9% clay	0.77 ± 0.04d	1.56 ± 0.14e

[a] Mean ± standard deviation of each analysis. Means within the same row and column followed by the same letters are not significantly different ($P < 0.05$); $n = 3$ for all treatments.

TABLE II
Effects of Starch Type on WVP of Starch-MMT Nanocomposite Films[a]

	WVP (g × mm/kPa × hr × m^2)		
MMT Content	**Corn Starch**	**Wheat Starch**	**Potato Starch**
0% MMT	1.61 ± 0.08a	1.73 ± 0.12ae	1.81 ± 0.15ah
3% MMT	1.42 ± 0.04b	1.35 ± 0.09bf	1.22 ± 0.10bi
6% MMT	1.06 ± 0.09c	0.94 ± 0.04cg	0.98 ± 0.06c–j
9% MMT	0.77 ± 0.04d	0.82 ± 0.08dg	0.84 ± 0.05dj

[a] Mean ± standard deviation of each analysis. Means within the same row and column followed by the same letters are not significantly different ($P < 0.05$); $n = 3$ for all treatments.

Generally, water vapor transmission through a hydrophilic film depends on both diffusivity and solubility of water molecules in the film matrix. When the nanocomposite structure is formed, the impermeable clay layers mandate a tortuous pathway for water molecules to traverse the film matrix, thereby increasing the effective path length for diffusion. The decreased diffusivity due to formation of intercalated nanostructure in starch-MMT composites reduced the WVP. On the other hand, addition of I30E did not lead to intercalated structure, thus there were no improvements in WVP of films made from starch-I30E composites.

Figure 9 shows the effect of 0–21% MMT on WVP of wheat starch-nanoclay composite films. WVP decreased sharply as clay content increased 0–6%. With further increase in MMT content to 21%, the WVP continued to decrease, although more gradually. WVP of wheat starch with 21% clay was 0.57 g × mm/kPa × hr × m^2, which was ≈70% lower than WVP of the wheat starch blank.

Table II and Fig. 10 show the effects of starch source and amylose content on WVP. Literature suggests that films made from different types of starches have different properties. Rindlav-Westling et al (1998) reported better barrier properties of high-amylose films compared with high-amylopectin films. Phan et al (2005) reported that the WVP of films is directly proportional to the amylopectin content. They suggested that the effect of the amylose content on the WVP of the starch could be attributed to the crystallization of amylose chains in the dried films. Amylose films showed B-type crystalline structure, whereas amylopectin films were completely amorphous. In general, diffusion of moisture is easier in amorphous systems than in crystalline systems. However, Table II shows that no significant difference in WVP was found between corn, wheat, and potato starch-based nanocomposite films using MMT, although there are some differences in starch granule size and shape, and amylose content between corn, wheat, and potato starches (Deis 1998). Regardless of starch sources, the WVP decreased with increase in clay content of 0–9%. In Fig. 10, normal corn starch-based films presented better barrier properties than either amylopectin or high-amylose-based nanocomposite films. When amylose content reached 50%, the WVP almost remained constant. This may be related to the XRD patterns. One reason is that the highest temperature used for extrusion processing was 120°C, which probably was not high enough for a higher degree of gelatinization of high-amylose starch. Knutson (1990) and Varavinit et al (2003) reported that

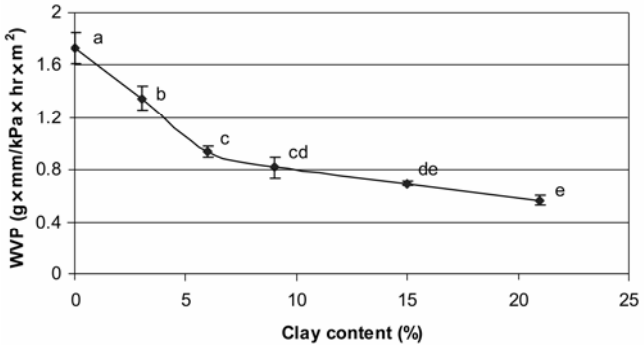

Fig. 9. Effects of clay (MMT) content on water vapor permeability (WVP) of wheat starch-based nanocomposite films. Error bars indicate standard deviation. Data points with different letters imply significant difference ($P < 0.05$).

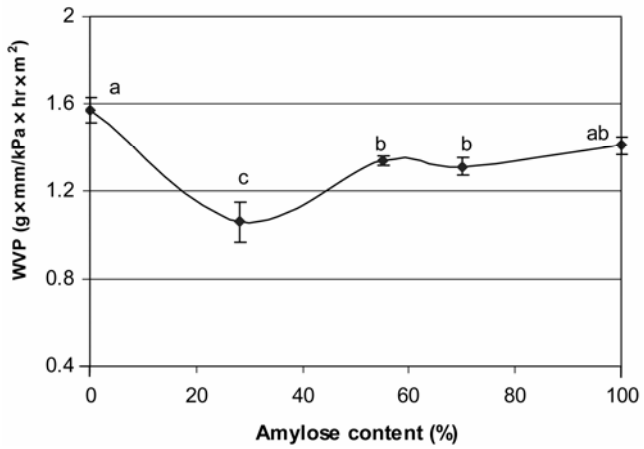

Fig. 10. Effect of amylose content on water vapor permeability (WVP) of corn starch-based nanocomposite films with 6% clay (MMT). Error bars ± SD. Data points with different letters imply significant difference ($P < 0.05$).

gelatinization temperatures increased with the increasing amounts of amylose. Bhattacharya and Hanna (1987) found that as the extruder barrel temperature increased from 116 to 164°C, % gelatinization increased from 73.6 to 98.4 in the waxy corn (1% amylose), while it increased from 40 to 55.2 in the ordinary corn samples (30% amylose) at the moisture content range of 17.8–42.2% (db). A higher degree of gelatinization means more disruption of starch granules and more leaching of amylose and amylopectin from the granule, thus facilitating the starch chains entering the clay galleries.

In addition, the presence of plasticizer (glycerol) may affect the film properties. Amylopectin was found to be more sensitive to glycerol plasticization than amylose in Lourdin et al (1995), who reported that the properties of plasticized films were not improved by the presence of glycerol and remained constant when amylose content was >40%. In addition, the presence of mineral clay may affect the starch network structure and crystallinity of amylose films.

Tensile Properties

Tables III–VI and Figs. 11 and 12 show the tensile properties of the starch-nanoclay composite films. Tensile properties such as TS and %E were evaluated from the experimental stress-strain curves obtained for all prepared nanocomposite films. Tables III and IV show the effects of clay type and clay content on tensile properties. When comparing TS of the starch/MMT and starch/I30E films (Table III), it was obvious that addition of natural MMT helped improve the TS of the films. TS increased with

the increasing of clay content. Similar to WVP, I30E still did not increase the TS of the films. For %E (Table IV), no trends and no significant difference could be found for the starch/MMT and starch/I30E films.

With increasing MMT content (Fig. 11), the TS increased rapidly from 14.05 to 27.02 MPa. However, %E did not exhibit much improvement. It even decreased with increased MMT content. This was coincident with the report by Lee et al (2005), which suggested that good dispersion of the clay platelets in the polymer reduced tensile ductility and increased tensile strength compared with neat polymer.

Theoretically, the complete dispersion of clay nanolayers in a polymer optimizes the number of available reinforcing elements for carrying an applied load and deflecting cracks. The coupling between the tremendous surface area of the clay and the polymer matrix facilitates stress transfer to the reinforcement phase, allowing for such tensile and toughening improvements.

Tables V and VI show TS and %E of different starch-based nanocomposite films. No significant differences of TS and %E were seen in nanocomposite films based on corn, wheat, and potato. Figure 12 shows the effects of amylose content on tensile properties. Amylose helps improve the mechanical properties of the films (Wolff et al 1951; Lourdin et al 1995). However, the results presented here were quite similar to those for WVP discussed above: regular corn-starch-based nanocomposite films presented the highest TS; the %E decreased with the increased amylose content; when amylose content was >50%, neither TS nor %E changed significantly.

TABLE III
Effects of Clay Type on Tensile Strength of Corn Starch-Based Films[a]

	Tensile Strength (MPa)	
Clay Content	**Starch-MMT**	**Starch-I30E**
0% clay	14.22 ± 0.98cd	14.22 ± 0.98d
3% clay	16.68 ± 2.32bc	12.41 ± 4.19cd
6% clay	18.60 ± 0.63b	13.37 ± 3.01d
9% clay	23.58 ± 0.58a	13.22 ± 1.35d

[a] Mean ± standard deviation of each analysis. Means within the same row and column followed by the same letters are not significantly different ($P < 0.05$); $n = 5$ for all treatments.

TABLE IV
Effects of Clay Type on %Elongation of Corn Starch-Based Films[a]

	Elongation at Break (%)	
Clay Content	**Starch-MMT**	**Starch-I30E**
0% clay	5.26 ± 0.83abc	5.26 ± 0.83c
3% clay	6.27 ± 1.20a	3.20 ± 0.81d
6% clay	4.44 ± 0.52b	4.51 ± 0.91bcd
9% clay	4.82 ± 0.35ab	4.99 ± 0.85ac

[a] Mean ± standard deviation of each analysis. Means with within the same row and column followed by the same letters are not significantly different ($P < 0.05$); $n = 5$ for all treatments.

TABLE V
Effects of Starch Type on Tensile Strength[a]

	Tensile Strength (MPa)		
Clay Content	**Corn Starch**	**Wheat Starch**	**Potato Starch**
0% clay	14.22 ± 0.98cd	14.05 ± 0.42dg	14.57 ± 0.41dk
3% clay	16.68 ± 2.32bc	16.21 ± 1.4cf	16.39 ± 0.30cj
6% clay	18.60 ± 0.63b	17.87 ± 1.4bf	18.66 ± 0.50bi
9% clay	23.58 ± 0.58a	21.27 ± 0.44e	22.25 ± 1.07eh

[a] Mean ± standard deviation of each analysis. Means with within the same row and column followed by the same letters are not significantly different ($P < 0.05$); $n = 5$ for all treatments.

TABLE VI
Effects of Starch Type on Elongation at Break[a]

	Elongation at Break (%)		
Clay Content	**Corn Starch**	**Wheat Starch**	**Potato Starch**
0% clay	5.26 ± 0.83abe	6.08 ± 0.6cde	5.47 ± 0.67e
3% clay	6.27 ± 1.20af	5.66 ± 1.49cdf	5.91 ± 0.73ef
6% clay	4.44 ± 0.52bh	7.86 ± 1.86cg	6.49 ± 0.61egh
9% clay	4.82 ± 0.35abj	5.09 ± 0.42dj	6.06 ± 0.58ei

[a] Mean ± standard deviation of each analysis. Means with within the same row and column followed by the same letters are not significantly different ($P < 0.05$); $n = 5$ for all treatments.

CONCLUSIONS

Biodegradable starch-clay nanocomposites were prepared by dispersing clay particles into the starch matrix through melt extrusion processing. Two types of clay, MMT and I30E, were chosen for the hybrid preparation. Starch/MMT showed better clay dispersion in the starch matrix. The dispersion of nanoclays in the starch matrix depended on the compatibility and the polar interactions among the starch, the silicate layers, and glycerol.

The starch/MMT composite films showed higher tensile strength and better barrier properties to water vapor than the starch/I30E hybrids, as well as the starch blank, due to the formation of intercalated or exfoliated nanostructure. Clay content had great effects on the properties of nanocomposite films. Higher TS and better barrier properties were obtained with increased clay content.

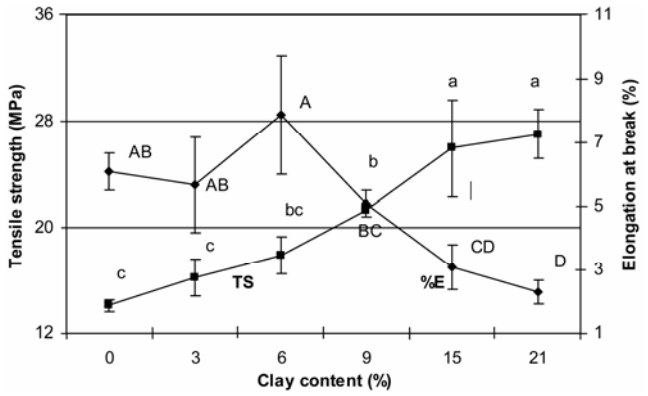

Fig. 11. Effects of clay content (MMT) on tensile properties of wheat starch-based nanocomposite films. Error bars ± SD. Data points with different letters imply significant difference ($P < 0.05$).

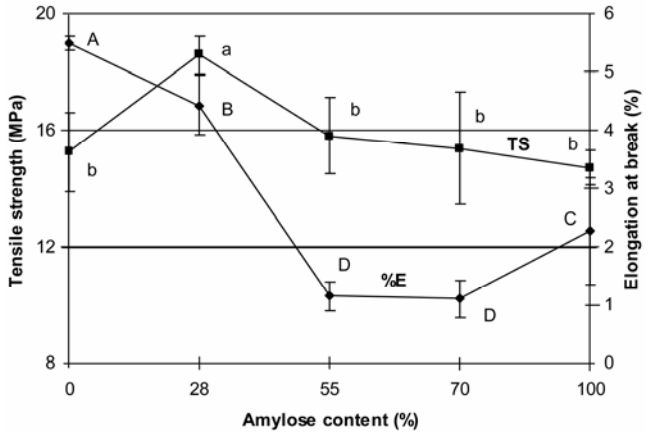

Fig. 12. Effect of amylose content on tensile properties of corn starch-based nanocomposite films with 6% MMT. Error bars ± SD. Data points with different letters imply significant difference ($P < 0.05$).

Normal corn starch-based films we studied here presented better barrier and mechanical properties than either the amylopectin or high-amylose-based nanocomposite films. WVP, TS, and %E values of the films did not change significantly as amylose content increased to >50%.

The results presented here for starch-MMT nanocomposites proved that the concept of nanocomposite technology can be applied to improve the properties of starch-based biopolymer. However, even better performance will be needed for extending its application. Further studies including influence of plasticizers and extrusion processing conditions on starch-MMT nanocomposites are currently underway.

ACKNOWLEDGMENTS

We would like to thank Eric Maichel, Operations Manager, KSU Extrusion Center, for conducting all extrusion runs. We also would like to thank KSU milling laboratory for providing milling facilities. This is Contribution No. 07-214-J from the Kansas Agricultural Experiment Station, Manhattan, KS 66506.

LITERATURE CITED

ASTM. 2000. Standard test method for the water vapor transmission of materials, E96-00. In: Annual Book of ASTM Standards. American Society for Testing and Material: Philadelphia.

ASTM. 2002. Standard test method for tensile properties of thin plastic sheeting, D882-02. In: Annual Book of ASTM Standards. American Society for Testing and Material: Philadelphia.

Avella, M., De Vlieger, J. J., Errico, M. E., Fischer, S., Vacca, P., and Volpe, M. G. 2005. Biodegradable starch/clay nanocomposite films for food packaging applications. Food Chem. 93:467-474.

Bhattacharya, M., and Hanna, M. A. 1987. Kinetics of starch gelatinization during extrusion cooking. J. Food Sci. 52:764-766.

Chen, L., Iman, S. H., Stein, T. M., Gordon, S. H., Hou, C. T., and Greene, R. V. 1996. Starch-polyvinyl alcohol cast film-performance and biodegradation. Polym. Prep. 37:461-462.

Chiou, B. S., Wood, D., Yee, E., Imam, S. H., Glenn, G. M., and Orts, W. J. 2007. Extruded starch-nanoclay nancomposites: Effects of glycerol and nanoclay concentration. Polym. Eng. Sci. 47:1898-1904.

De Carvalho, A. J. F., Curvelo, A. A. S., and Agnelli, J. A. M. 2001. A first insight on composites of thermoplastic starch and kaolin. Carbohydr. Polym. 45:189-194.

Deis, R. C. 1998. The new starches. Food Product Design. Available online at www.foodproductdesign.com/articles/463/463_0298CS.

Doane, W. M. 1994. Opportunities and challenges for new industrial uses of starch. Cereal Foods World 39:556-563.

El Amin, A. 2005. Common plastics packaging chemical linked to cancer. FoodProductionDaily e-newsletter. Available at http://www. foodproductiondaily.com/news/ng.asp?id=60333-common-plastics-packaging

Giannelis, E. P. 1996. Polymer layered silicate nanocomposites. Adv. Mat. 8:29-35.

Huang, M., Yu, J., and Ma, X. 2006. High mechanical performance MMT-urea and formamide-plasticized thermoplastic cornstarch biodegradable nanocomposites. Carbohydr. Polym. 63:393-399.

Ke, T., and Sun, X. 2000. Physical properties of poly(lactic acid) and starch composites with various blending ratios. Cereal Chem. 77:761-768.

Kirsch, C. 2005. Compounds in plastic packaging act as environmental estrogens altering breast genes. EurekAlert e-newsletter. Available at http://www.eurekalert.org/pub_releases/2005-04/fccc-cip041405.php.

Knutson, C. A. 1990. Annealing of maize starches at elevated temperatures. Cereal Chem. 67:376-384.

Kojima, Y., Usuki, A., Kawasumi, M., Okada, A., Fukushima, Y., Kurauchi, T., and Kamigaito, O. 1993a. Mechanical properties of nylon 6-clay hybrid. J. Mater. Res. 8:1185-1189.

Kojima, Y., Usuki, A., Kawasumi, M., Okada, A., Kurauchi, T., and Kamigaito, O. 1993b. Sorption of water in nylon 6-clay hybrid. J. Appl. Polym. Sci. 49:1259-1264.

Krochta, J. M., and De Mulder-Johnston, C. 1997. Edible and biodegradable polymer films: Challenges and opportunities. Food Technol. 51:61-74.

Kurokawa, Y., Yasuda, H., and Oya, A. 1996. Preparation of a nanocomposite of polypropylene and smectite. J. Mater. Sci. Lett. 15:1481-1483.

Lee, J. H., Jung, D., Hong, C. E., Rhee, K. Y., and Advani, S. G. 2005. Properties of polyethylene-layered silicate nanocomposites prepared by melt intercalation with a PP-g-MA compatibilizer. Compos. Sci. Technol. 65:1996-2002.

Lourdin, D., Della Valle, G., and Colonna, P. 1995. Influence of amylose content on starch films and foams. Carbohydr. Polym. 27:261-270.

Ma, X., Yu, J., and Feng, J., 2004. Urea and formamide as a mixed plasticizer for thermoplastic starch. Polymer Int. 53:1780-1785.

Mani, R., Tang, J., and Bhattacharya, M. 1998. Synthesis and characterization of starch-graft-polycaprolactone as compatibilizer for starch and polycaprolactone blends. Macromolec. Rapid Com. 19:283-286.

McGlashan, S. A., and Halley, P. J. 2003. Preparation and characterization of biodegradable starch-based nanocomposite materials. Polym. Int. 52:1767-1773.

Pandey, J. K., and Sing, R. P. 2005. Green nanocomposites from renewable resources: Effect of plasticizer on the structure and material properties of clay-filled starch. Starch 57:8-15.

Park, H., Li, X., Jin, C., Park, C., Cho, W., and Ha, C. 2002. Preparation and properties of biodegradable thermoplastic starch/clay hybrids. Macromol. Mater. Eng. 287:553-558.

Park, H., Lee, W., Park, C., Cho, W., and Ha, C. 2003. Enviromentally friendly polymer hybrids. 1. Mechanical, thermal and barrier properties of thermoplastic starch/clay nanocomposites. J. Mater. Sci. 38:909-915.

Phan, D., Debeaufort, F., Luu, D., and Voilley, A. 2005. Functional properties of edible agar-based and starch-based films for food quality preservation. J. Agric. Food Chem. 53:973-981.

Rindlav-Westling, A., Stading, M., Hermansson, A. M., and Gatenholm, P. 1998. Structure, mechanical and barrier properties of amylose and amylopectin films. Carbohydr. Polym. 36:217-224.

Sinha Ray, S., Yamada, K., Okamoto, M., and Ueda, K. 2002a. New polylactide/layered silicate nanocomposite: A novel biodegradable material. Nano Lett. 2:1093-1096.

Sinha Ray, S., Maiti, P., Okamoto, M., Yamada, K., and Ueda, K. 2002b. New polylactide/layered silicate nanocomposites. 1. Preparation, characterization and properties. Macromolecule 35:3104-3110.

Sinha Ray, S., and Okamoto, M. 2003. Polymer/layered silicate nanocomposites: A review from preparation to processing. Prog. Polym. Sci. 28:1539-1641.

Tharanathan, R. N. 2003. Biodegradable films and composite coatings: Past, present and future. Trends Food Sci. Technol. 14:71-78.

Usuki, A., Kato, M., Okada, A., and Kurauchi, T., 1997. Synthesis of polypropylene-clay hybrid. J. Appl. Polym. Sci. 63:137-139.

Vaia, R. A., and Giannelis, E. P. 1997. Polymer melt intercalation in organically-modified layered silicates: Model predictions and experiment. Macromolecules 30:8000-8009.

Vaia, R. A., Jandt, K. D., Kramer, E. J., and Giannelis, E. P. 1995. Kinetics of polymer melt intercalation. Macromolecules 28:8080-8085.

Varavinit, S., Shobsngob, S., Varanyanond, W., Chinachoti, P., and Naivikul, O. 2003. Effect of amylose content on gelatinization, retrogradation and pasting properties of flours from different cultivars of Thai rice. Starch 55:410-415.

Wilhelm, H. M., Sierakowski, M. R., Souza, G. P., and Wypych, F. 2003. Starch films reinforced with mineral clay. Carbohydr. Polym. 52:101-110.

Wolff, I. A., Davis, H. A., Cluskey, J. E., Gundrum, L. J., and Rist, C. E. 1951. Preparation of films from amylose. Indus. Eng. Chem. 43:915-919.

[Received October 11, 2007. Accepted December 18, 2007.]